GeoVirtual 2020 September 14-16
Resilience and Innovation

Monitoring of the change of moisture beneath a railway embankment and the effectiveness of a wicking geotextile

Camila Alvarenga, Parisa Haji Abdulrazagh, Michael T. Hendry

Faculty of Engineering – University of Alberta, Edmonton, Alberta, Canada

ABSTRACT

A 45 m section of railway embankment was remediated on Canadian Pacific Railway's (CP) Scotford subdivision to address issues of ongoing settlement and mud pumping. The track panel and embankment materials were replaced with new materials inclusive of a geotextile between the ballast and sub-ballast layers, and a wicking geotextile between the subgrade and sub-ballast. 5TE moisture sensors are installed at both the remediated section and an adjacent control section, along with access pipes for the use of a "Diviner 2000" probe to measure profiles of moisture with depth. This paper presents a comparison of the trends of volumetric water content (VWC) versus time between the two adjacent sites. The results are used to study the impact of precipitation events on VWC of soils and to interpret the effect of VWC on the unsaturated strength of the soil based on SWCC results. The early results of moisture-suction relationship shown that the strength of the subgrade material in the remediated section is improving; however, these trends are anticipated to be clearer with a full year of measurements.

RÉSUMÉ

Un tronçon de 45 m de remblai ferroviaire a été assaini dans la subdivision Scotford de CP afin de régler les problèmes de tassement et de pompage de boue. Le panneau de voie et les matériaux de remblai ont été remplacés par de nouveaux matériaux comprenant un géotextile entre les couches de ballast et de sous-ballast, et un géotextile à effet de mèche entre le sol de fondation et le sous-ballast. Des capteurs d'humidité 5TE sont installés à la fois dans la section assainie et dans une section de contrôle adjacente, ainsi que des tubes d'accès pour l'utilisation d'une sonde «Diviner 2000» pour mesurer les profils d'humidité en profondeur. Cet article présente une comparaison des tendances de la teneur en eau volumétrique (VWC) en fonction du temps entre les deux sites adjacents. Les résultats sont utilisés pour étudier l'impact des événements de précipitations sur la VWC des sols et pour interpréter l'effet de la VWC sur la résistance insaturée du sol sur la base des résultats du SWCC. Les premiers résultats de la relation humidité-aspiration ont montré que la résistance du matériau de fondation dans la section assainie s'améliore; cependant, ces tendances devraient être plus claires avec une année complète de mesures.

1 INTRODUCTION

Railways in Canada make an essential contribution to the economy, transportation of goods and people throughout the country. As recognized by several authors (Indraratna et al, 2011; Li et al, 2002; Rushton and Ghataora, 2014), drainage is one of the major aspects of the railway design, and site conditions such as the soil profile and local climatic factors must be considered.

Water accumulation is a common cause of track substructure problems, leading to several issues such as pumping of fine-grained soils, track settlement, soil volume change, ballast degradation, frost heave/thaw softening and cess heave due to strength reduction, all of these causing a decrease in the serviceable lifespan of the track and increasing considerably the maintenance costs. Railway tracks founded on clays and silts tend to be the focus of most subgrade improvement work (Indraratna et al, 2011: Li et al, 2002)

An additional countermeasure to resolve the aforementioned problems is the use of geosynthetics where ground improvement is necessary. According to Koerner (2006), the use of geosynthetics aims to improve the soil in a more economical way when compared to traditional materials, and it serves to multiple functions such as separation, reinforcement, filtration and drainage improvement.

According to Wang et al (2016), Mirafi® H2Ri enables lateral drainage of the embankment materials through the use of capillary action within deep grooved wicking fibers woven into a geotextile; thus, reducing the accumulation of moisture in the embankment materials

and subgrade soils. The manufacturer recommends this geotextile for subgrade stabilization of roads, railways and airports.

The focus of this study is to monitor the moisture retention beneath railway embankments, and to evaluate the impact of embankment reconstruction along with the introduction of wicking geotextiles, on the levels of moisture and strength of the subgrade soils beneath railway embankments.

2 MATERIALS AND METHODS

2.1 Site Description

The research site is located at CP's Scotford subdivision near Fort Saskatchewan County in Alberta. The railway subgrade soil is composed of 17% clay, 26% silt, 37% sand and 20% gravels. Previously, the track presented issues such as settlement and pumping of fines, attributed to poor drainage and retention of moisture within both the embankment and subgrade.

The study site consists of two sections of track, one as a control (unchanged) and the second underwent remediation. The remediation consisted of removing the track, excavating the embankment and disturbed subgrade material, then reconstructing the embankment with clean ballast, sub-ballast and geotextiles as per Fig. 1. The length of the remediated site was 36 m (118 ft.). The control section did not undergo any changes, except for the installation of the monitoring system.

This site provided the opportunity of monitoring the seasonal changes of moisture content within the subgrade at a site with known drainage issues, while also evaluating the effectiveness of the chosen remediation methods. A comparison of remediations with and without the wicking geotextile was not an option for this study. In order to monitor the VWC along both sections, moisture sensors were installed at the centerline of the subgrade, at the centerline and at the shoulders of the sub-ballast layer.

It was expected that the remediation would lower the moisture content of the subgrade and embankment materials, thus leading to a decrease in the pumping of fines from subgrade and soil strength retention.

2.2 Specification of Geotextiles

Two geotextiles were installed at the remediated site. The first geotextile (Mirafi® RS580i) is shown as a solid pink line in the interface of ballast and sub-ballast layer in Fig. 1. The function of this woven geotextile is soil reinforcement and confinement (Tencate Geosynthetics, 2018). The green solid line in the interface of sub-ballast and subgrade represents the location of Mirafi® H2Ri. This wicking geotextile has hydrophilic and hygroscopic wicking yarns woven in the textile, which are responsible for reducing water accumulation through capillary effect (Wang et al, 2016). Mirafi® RS580i and Mirafi® H2Ri mechanical and hydraulic properties can be found in Tencate Geosynthetics (2018) and Tencate Geosynthetics (2015), respectively. These two types of geotextiles were used by CP for local remediation.

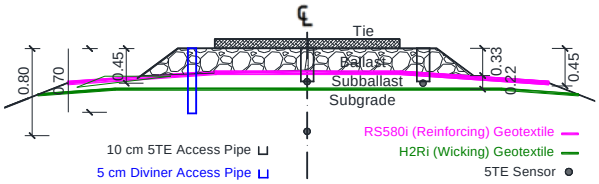

Figure 1. Location of reinforcing (Mirafi® RS580i) and wicking (Mirafi ® H2Ri) geotextiles).

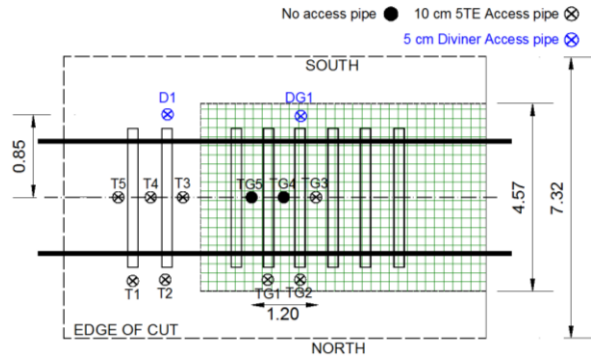

Figure 2. Plan view of instrumentation (dimensions in m).

2.3 Site Instrumentation

Ten 5TE moisture sensors were placed at both sections for the investigation. These sensors measure bulk electrical conductivity, volumetric water content (VWC) and soil temperature making use of an oscillator running at 70 MHz in order to measure the dielectric permittivity of the soil. The installation setup is shown in Fig. 2, where the sensors installed at the control section are named "T" and the sensors installed at the remediated area are defined as "TG". In each section, two sensors were installed in the shoulder and one in the centerline of sub-ballast at a depth of 0.45 m from the ballast surface level; and two sensors were placed 0.70 m deep in the centerline of the subgrade layer. The location and depth of sensors are presented in Fig. 1 and Table 1. All the sensors at the control site were installed after the placement of access pipes. However, in the remediated section, the sensors in the subgrade were placed during the reconstruction process and no access pipes were inserted at that time (Figs. 2 and 3).

Two data loggers were installed at the research site, one for the control site and one for the remediated section. For remediated section construction, the track panel was removed to perform an excavation of the pre-existing ballast and sub-ballast in the length of 36 m (118 ft). A trench was excavated for the insertion of sensors in the subgrade section, being backfilled afterwards. The wicking geotextile was installed on the top of the subgrade, followed by the placement of sub-ballast, ballast and the track panel.

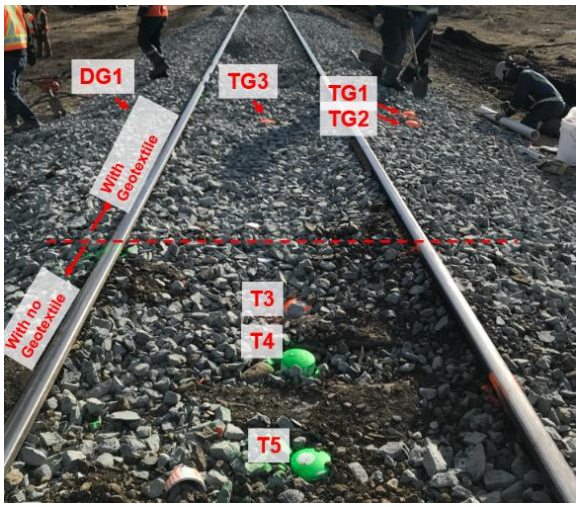

Figure 3. Location of installed access pipes in the middle and shoulders of track at controlled and remediated sections.

Table 1. Location of 5TE sensors and Diviner access pipes.

Sensor	Depth (m)	Position at Track	Section	Color
TG1/ TG2	0.45	Shoulder	Remediated	Orange
TG3	0.45	Centreline	Remediated	Orange
TG4[1]	0.80	Centreline	Remediated	-
TG5	0.80	Centreline	Remediated	-
T1/ T2	0.45	Centreline	Control	Green
T3	0.45	Shoulder	Control	Green
T4	0.65	Centreline	Control	Green
T5	0.80	Centreline	Control	Green
D1	0.60	Shoulder	Control	White
DG1	0.70	Shoulder	Remediated	White

[1] Sensor is not functional.

The 5TE moisture sensors installed at the track substructure were connected to two dataloggers configured to read soil temperature, bulk electrical conductivity and VWC at 12-hour intervals. The Diviner 2000® is a portable soil moisture probe manufactured by Sentek Sensor Technologies. The system uses frequency domain reflectometry (FDR) to obtain near continuous moisture readings throughout the soil profile at 0.1 m (4 inches) intervals up to a depth of 1.6 m (5 ft) (Sentek, 2004). The probe is connected to a portable display unit which records moisture profiles that can be downloaded to a laptop computer. The measurements are done through the wall of PVC access pipes. One access pipe was placed at each section, going down to the subgrade layer. The reading of VWC by Diviner 2000 started in October 2019. The access pipes are denoted as “D1” and DG1” in Fig. 2.

2.4 Climate Data Acquisition

Meteorological data was acquired in the ECCC (2019) website, using measurements from three different weather stations that are within 25 km of the site. One station is located at 6.06 km from the site which provided daily air temperature, rainfall, snowfall and total precipitation. Since there were some months without precipitation data at the first station, data was also collected at a second station (located at 21.57 km from the site) only for the 10-year average calculation. The third station is at a distance of 18.34 km and provided more complete maximum, minimum and mean air temperature data. Temperature and precipitation values from the years 2008-2018 were used (Figs. 4 and 5) to determine the historical profile of the region, as well as the profile for 2019-2020, that have shown an unusual amount of precipitation during the summer and a greater amount of rainfall during October and November than anticipated. The average temperatures during the study were similar to the 10-year average.

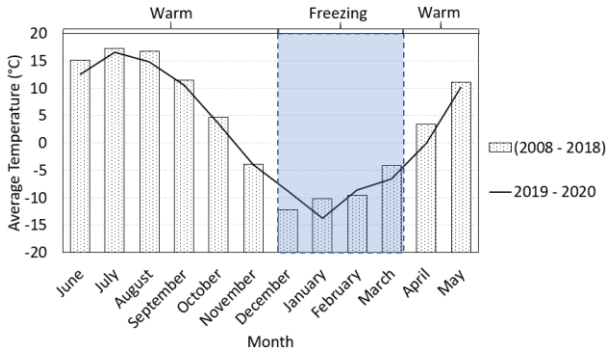

Figure 4. 10-year average temperature (2008-2018), vs. recorded temperatures (2019-2020) (data from ECCC (2019)).

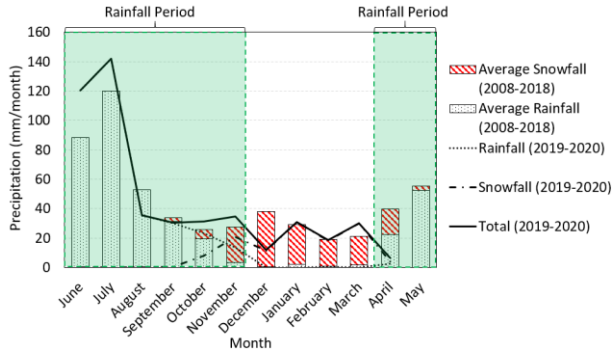

Figure 5. 10-year average precipitation (2008- 2018) vs. recorded precipitation (2019 and 2020) (data from ECCC (2019)).

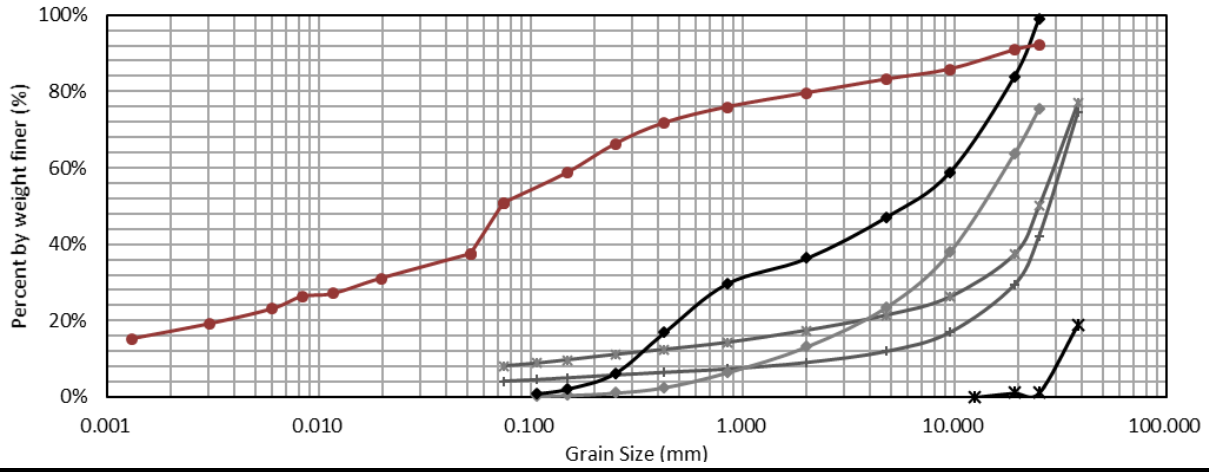

Sample	Location	Symbol	Depth (m)	D_{10} (mm)	D_{30} (mm)	D_{60} (mm)	Passing #200 (w)	Sand	Gravel	GWC	LL	PL	PI	Gs
Ballast top	Control		0.25	3	19.7	31.8	4.1%	3.9%	92.0%	2.3%	-	-	-	-
Ballast bottom	Control		0.33	0.17	12.5	29.4	8.1%	9.3%	82.6%	3.7%	-	-	-	-
Sub-ballast	Control		0.5	1.36	6.9	17.5	0.3%	12.7%	87.0%	4.2%	-	-	-	2.71
Ballast	Remediated		0.3	31.5	-	-	0%	0.0%	100.0%	0.2%	-	-	-	-
Sub-ballast	Remediated		0.5	0.31	0.87	10	0.1%	35.6%	63.5%	3.6%	-	-	-	2.68
Subgrade	Remediated and Control		0.8	-	0.017	0.165	50.1%	28.7%	20.5%	20.6%	40	19	21	2.73

Figure 6. Material characterization for railway embankment materials.

The historical data was important to decide when snow accumulation would occur, what would influence directly the accuracy of the antecedent precipitation index (API) model (Section 4.4).

3 SOIL CHARACTERIZATION

Some of the factors that may influence the moisture-suction relationship are the percentage of clay, the particle size, texture and specific surface. Sieve analysis, moisture content, specific gravity, and Atterberg limits tests were performed to understand the soil behaviour and to verify the applicability of the method presented. Three tests were performed for each type of soil and averaged when possible, except for the moisture content and particle size distribution (PSD) tests that had one test performed per soil type due to sample availability.

As the control section did not have its sub-ballast and ballast substituted, tests were performed for the materials of each section, except for the subgrade, that is the same for both sections. The control section will have its materials identified with “CS”, while the remediated section materials will be identified with “RS”.

Figure 6 shows the particle size distribution for each soil tested. The ballast and sub-ballast at the control site had a “transition” layer on their interface, therefore leading to the presence of sand in the ballast. Clean ballast was used in the remediated section. For the control section, both ballast and sub-ballast have shown less than 10% of fine materials. The subgrade had the greatest percentage of fines of all layers (approximately 50%).

Gravimetric moisture content tests were performed in all materials to check field conditions, and its results are summarized in the column “GWC” in the table shown in Fig. 6. The top layer of the remediated section has shown a moisture content of less than 1%, while for the control section, the average found was 3% due to the presence of some of the sub-ballast material. The sub-ballast material has shown a moisture content between 3 and 4% for both sections.

Soil water characteristic curves (SWCCs) were applied to estimate the in-situ suction, as it defines the relationship between VWC and matric suction, providing a function which is often used for the evaluation of unsaturated soil properties. There are two points along the curve that are crucial: the “air-entry value” of the soil and “residual conditions”. (Fredlund et al., 2012).

The Zapata (1999) correlations for plastic materials were used for the estimation of the SWCC of the subgrade shown in Fig. 7 due to time constraint. In this correlation, the fitting parameters (i.e., a_f, m_f, n_f, and h_r) are estimated using percent passing the No. 200 sieve (represented as w) multiplied by the plasticity index of the soil (PI) as shown by Eq. 1, 2 3 and 4.

$$a_f = 0.00364(wPI)^{3.35} + 4(wPI) + 11 \quad [1]$$

$$m_f = 0.0514(wPI)^{.465} + 0.5 \quad [2]$$

$$n_f = m_f(-2.313(wPI)^{0.14} + 5 \quad [3]$$

$$h_r = a_f\left(32.44e^{0.0186(wPI)}\right) \quad [4]$$

The estimated parameters were then processed using SVOffice 5 to provide the SWCC according to Fredlund and Xing (1994) equation:

$$\theta(\psi) = C(\psi)\frac{\theta_s}{\{\ln[e + (\psi/a_f)^{n_f}]\}^{m_f}} \quad [5]$$

Where a_f, n_f and m_f are fitting parameters, θ is the VWC corresponding to a selected soil suction, θ_s is the saturated VWC, ψ is the suction, e is equal to 2.72, $C(\psi)=1-\{\ln[1+ \psi/ \psi_r]/\ln[1+1000000/ \psi_r]\}$ is the correction factor and ψ_r is the suction at the residual value.

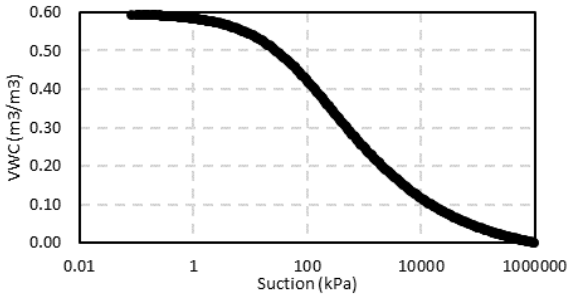

Figure 7. Soil-water characteristic curve for subgrade material.

4 RESULTS AND DISCUSSION

4.1 Sensors Performance

During July 2019- April 2020, the data acquired by the moisture sensors were recorded at an interval of 12 hours. The data collection, the sensors and the dataloggers' functionality were checked monthly. Sensor TG4 was damaged during the construction of the embankment and does not function. This sensor is inaccessible, as it was installed at a trench before the track reconstruction to avoid the cut through reinforcing and wicking geotextiles. No data were collected between July 24, 2019 and September 19, 2019 for the control section due to datalogger malfunction.

4.2 Diviner 2000 Measurements

Measurements of VWC with depth were collected with the Diviner on Nov. 1, 2019; Nov. 19, 2019; Dec. 13, 2019; Jan. 30, 2020 and Apr.17, 2020 through the access pipes installed at the shoulder of the track. Except for Apr. 17, 2020, it was not possible to perform measurements below 55 cm at the remediated section due to presence of water/ice at the base of the Diviner access pipes, even though the hole is 70cm deep.

As shown in Fig. 9, the Diviner has shown considerably lower values of VWC, which could be due to the original calibration of the probe. The 5TE readings from the same days have shown higher VWC values, mainly in the last 20 cm. Low VWC values (<10%) were found for the bottom layers of the remediated section with the Diviner, a trend that is not seen in the 5TE sensors (Figs. 13(a) and 13(b)). The groundwater table is not believed to be the reason for a higher VWC in the subgrade, since *in situ* tests showed it was placed at a 7 m depth from the subgrade material.

4.3 VWC Measurements

Short term fluctuations of VWC between 12-hour readings were negligible. Sensors at the shoulder (T1, T2, TG1 and TG2) measured greater moisture content in the remediated section through July – Nov. 2019. Nonetheless, sharp changes in the moisture caused by precipitation were more prominent for the control site, suggesting a greater influence of precipitation at this section. The sensors at the sub-ballast centerline (T3 and TG3) have shown similar VWC for both sections, but the response to precipitation at the remediated section seems to be less pronounced than for the control section (Fig. 8).

At the subgrade layer, the remediated section showed considerably lower results of VWC at all times, with a difference of about 9%. However, the site construction using dryer material on top might have reduced the *in-situ* water content. VWC at the remediated section appears to be more responsive to periods of less precipitation, as a slight reduction in VWC is seen during dry periods. At the time of the study, no significant changes occurred in the VWC at the control section.

It is yet to be determined whether this solution makes a great impact on the VWC found after the spring thaw, which started mid-April. It is also necessary to monitor the soil behaviour through the summer for a more comprehensive analysis.

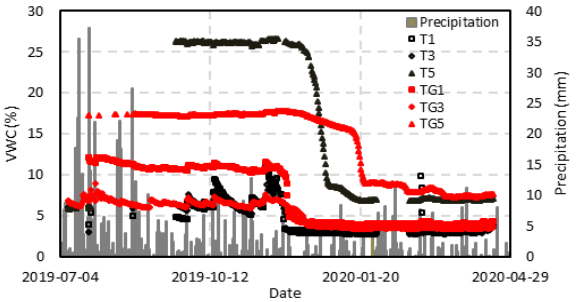

Figure 8. Variation of VWC with precipitation.

4.4 VWC Model with API

The soil water content is influenced by many environmental factors, such as soil properties,

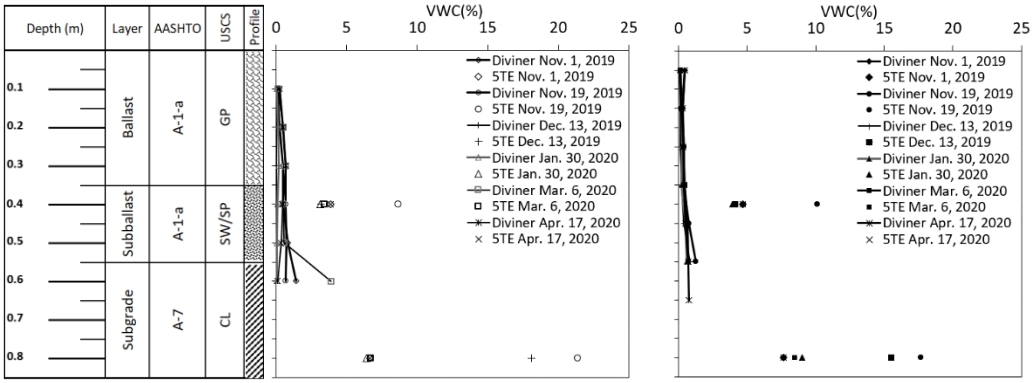

a) b)

Figure 9. Diviner vs. 5TE measurements for a) Control section and b) Remediated section.

topography, vegetation, precipitation, evapotranspiration, temperature and wind speed (Gwak and Kim, 2016). However, it is difficult to consider all those variables in the change of moisture.

The interrelationship between precipitation and VWC at a daily scale is studied in this section by developing an API model. The development of this model facilitates the understanding of the correlation between the precipitation data available from the weather stations and the VWC measurements obtained from the 5TE sensors. The API model was used to understand the trend of VWC only by acquiring precipitation data. API can be defined by Eq. 6 (Kohler and Linsley, 1951)

$$API_t = \sum_{t=0}^{d} P_t k^t \qquad [6]$$

Where P_t is the precipitation at day t, k is the attenuation coefficient (0< k <1) and t refer to time in days. The attenuation coefficient was estimated for each layer according to the best curve fitting value (Tables 2 and 3).

The period chosen for the VWC data analysis goes from July 23 - Nov. 4, 2019, considering snow accumulation occurred after this date. The interference of snow would influence the accuracy of API, since precipitation could not fully penetrate the ground. Nevertheless, the control section only had data recorded after Sept. 19, 2019 as a result of an issue with the datalogger. A sensitivity analysis showed that the trend seen for both cases would not be greatly affected by the amount of input for each section.

Graphical interpretation was performed in VWC vs. API for each sensor applying the power regression model shown in Eq. 7, previously used by Blanchard et al. (1981).

$$\theta_{v(t)} = \alpha API_t^{\beta} \qquad [7]$$

Where α and β are fitting parameters, and $\theta_{v(t)}$ is the estimated VWC for day t. The parameters for each sensor are described in Table 2, and examples of the curve fitting performed are shown in Figs. 10 and 11. The curve determined for each sensor was afterwards used to estimate VWC according to daily API (Fig. 13(a)-13(d)). The calculated coefficient of determination (R-squared value) between the estimated VWC and actual VWC is between 0.36 and 0.85 in Tables 2 and 3.

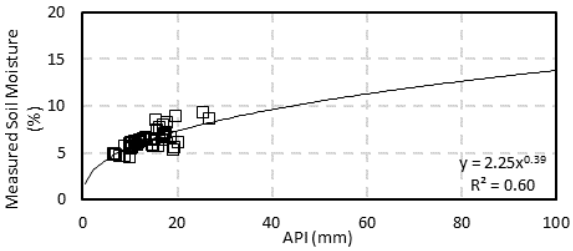

Figure 10. Curve-fitting with power regression function for T1 sensor at control section.

Table 2. Curve-fitting parameters for control section.

Sensor	Layer	k	# Days	Fitting Curve	R^2
T1	Sub-ballast	0.96	23	$2.25*API_t^{0.3939}$	0.60
T2	Sub-ballast	0.96	23	$3.87*API_t^{0.1480}$	0.44
T3	Sub-ballast	0.96	15	$5.05*API_t^{0.1061}$	0.39
T4	Subgrade	0.95	28	$5.78*API_t^{0.3357}$	0.61
T5	Subgrade	0.95	32	$26.68*API_t^{0.007}$	0.36

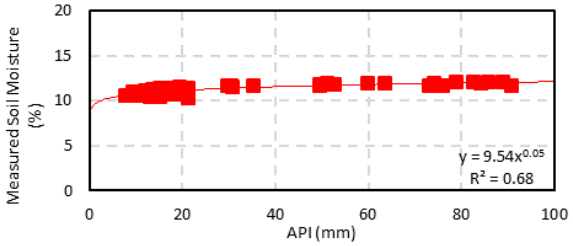

Figure 11. Curve-fitting with power regression function for TG1 sensor at remediated section.

Table 3. Curve-fitting parameters for remediated section.

Sensor	Layer	k	# Days	Fitting Curve	R^2
TG1	Sub-ballast	0.96	22	$9.55*API_t^{0.0529}$	0.85
TG2	Sub-ballast	0.96	22	$7.87*API_t^{0.0429}$	0.42
TG3	Sub-ballast	0.96	13	$5.83*API_t^{0.0524}$	0.51
TG5	Subgrade	0.95	33	$16.94*API_t^{0.0087}$	0.36

Values found for β in Tables 2 and 3 show how moisture is changing in each layer. Lower values for β indicate a less pronounced response to precipitation, which is seen for the sensors at the sub-ballast layer in the remediated section. The sensors at the sub-ballast shoulder of the remediated section displayed higher VWC than those in the control section (Figs. 13(a) and (b)). However, the VWC at the remediated section appears to be less influenced by precipitation (β_{TG1}=0.0529, β_{TG2}=0.0429 in Table 3) than the control section (β_{T1}=0.3939, β_{T2}=0.1480 in Table 2).

VWC data for the subgrade material did not show sharp changes, but the variation of recordings by TG5 sensor in the remediated section is greater than those recorded in the control section (Fig. 13(d)). As precipitation decreased, the sensor in the subgrade (TG5) has shown a slight decrease in its VWC accordingly (βT_{G5}=0.0087 in Table 3). In contrast, the VWC remained constant throughout the test period at the control section (T5), and displayed a weak relationship with API, indicated by the negative value of β_{T5}=-0.007 (Table 2). This rather contradictory result may reflect the occurrence of water retention in the control section when compared to the remediated section.

The number of days affecting the VWC measurements for each layer were defined according to the best fit in Tables 2 and 3. The estimated day range that affects the VWC of the subgrade and sub-ballast in the remediated section are close to the ones found for the control section, staying within a difference of 2 days.

4.5 Soil Strength Analysis

The effect of the inclusion of the wicking geotextile and VWC variation on the strength of subgrade material is observed in terms of matric suction in this section. The contribution of the matric suction to the soil shear strength can be visualized using Eq. 8, developed by Fredlund et al. (1978):

$$\tau = c' + (\sigma - u_w)\, tan\varphi' + (u_a - u_w)\, tan\varphi^b \qquad [8]$$

Where τ is the shear strength, c′ is the effective cohesion; σ is the total normal stress, (u_a – u_w) is the matric suction, u_w is the pore-water pressure and φ′ is the friction angle with respect to changes in (σ – u_w) when (u_a – u_w) is held constant; and φ^b is the friction angle with respect to changes in (u_a – u_w) when (σ – u_w) is held constant. The unsaturated conditions cause the development of a third component that considers the suction effect on the soil, which leads to an increase in the shear strength and a consequent improvement in the bearing capacity of the material.

Associating the VWC readings from July 23, 2019 to Dec. 1, 2019 with the SWCC curve shown in Fig. 7 made possible to estimate the field suction values found for both sections in the subgrade layer. The lower VWC values found in the remediated section contributed significantly to the estimated suction values (Fig. 12). A difference of 9% between the VWC found for both sections caused the matric suction to go from 747 kPa in the control section to 3056 kPa in the remediated section, demonstrating that the wicking geotextile could be improving the soil strength. However, this interpretation must be treated with caution as these results do not rule out the influence of other factors, such as the impact of the construction method and different PSD for the sub-ballast layer of both sections.

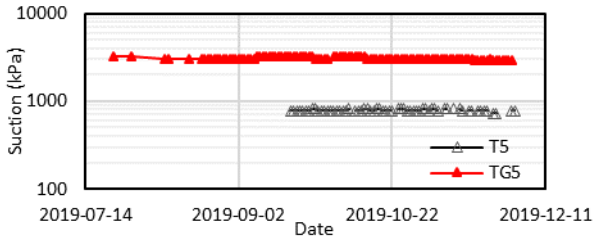

Figure 12. Suction values for control (T5) and remediated section (TG5).

5 CONCLUSIONS

The use of adjacent sites for the study allowed a direct comparison of the performance of the wicking geotextile to a common setup. These early results indicate that despite of the higher recorded VWC values in the sub-ballast shoulder for the remediated section in contrast to those found for the control section, the API model (lower β-values) indicates that the sub-ballast layer at the remediated section tends to be less sensitive to the antecedent precipitation. The curve-fitting values for β in the API model displayed a better relationship to precipitation for the subgrade in the remediated section rather than the control section. This trend might be attributed to the fact that the subgrade in the remediated section appears to retain less water, and releases moisture accordingly as precipitation ceases.

Greater suction values of subgrade material in the remediated section may be due to the reduced VWC found. The analysis will be continued to determine how the geotextile will affect the studied section during spring thaw season and in a long-term.

6 ACKNOWLEDGEMENT

This research was made possible through the support of the Railway Ground Hazard Research Program, funded in part by the Natural Sciences and Engineering Research Council of Canada (NSERC), Canadian Pacific and Canadian National Railway.

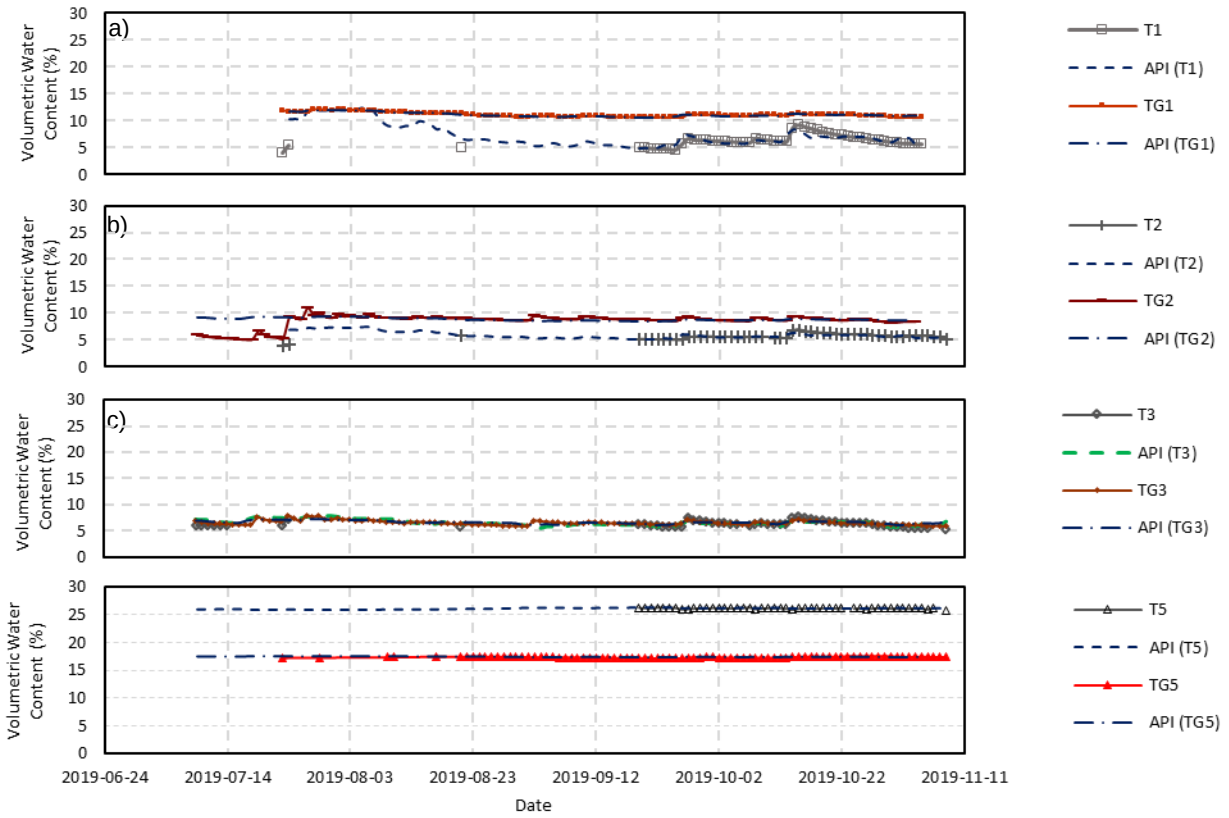

Figure 13. Soil moisture content measurements and API model for a) and b) Sub-ballast shoulder, c) Sub-ballast centerline and d) Subgrade centerline.

7 REFERENCES

Blanchard, B. J., Mcfarland, M. J., Schmugge, T. J., & Rhoades, E. (1981). Estimation of Soil Moisture with API Algorithms and Microwave Emission. Journal of the American Water Resources Association, 17(5), 767–774. DOI: 10.1111/j.1752-1688.1981.tb01296.

Environment and Climate Change Canada (ECCC) (2019). Historical Data: 2008-2018. Accessed April 09, 2020, from https://climate.weather.gc.ca/historical_data/search_historic_data_e.html.

Fredlund, D. G., Morgenstern, N. R., & Widger, R. A. (1978). The shear strength of unsaturated soils. Accessed April 17, 2020, from https://www.nrcresearchpress.com/doi/10.1139/t78-029.

Fredlund, D. G., Rahardjo, H., & Fredlund, M. D. (2012). *Unsaturated Soil Mechanics in Engineering Practice*. New York, NY: John Wiley & Sons Inc. DOI: 10.1002/9781118280492.

Gwak, Y., & Kim, S. (2016). Factors affecting soil moisture spatial variability for a humid forest hillslope. Accessed April 20, 2020, from https://onlinelibrary.wiley.com/doi/abs/10.1002/hyp.11039.

Indraratna, B., Salim, W., & Rujikiatkamjorn, C. (2011). Advanced Rail Geotechnology: Ballasted Track (1st ed.). Boca Raton: CRC Press/Taylor & Francis Group. https://doi.org/10.1201/b10861.

Kohler, M. A., & Linsley, R. K. (1951). Predicting the Runoff from Storm Rainfall. Accessed April 18, 2020, https://www.nrc.gov/docs/ML0819/ML081900279.pdf.

Li, D., Hyslip, J., Sussmann, T., & Chrismer, S. (2002). Railway Geotechnics (1st ed.). London: CRC Press. https://doi.org/10.1201/b18982.

Rushton, K. R., & Ghataora, G. (2014). Design for efficient drainage of railway track foundations. In Proceedings of the Institution of Civil Engineers-Transport (Vol. 167, No. 1, pp. 3-14). Thomas Telford Ltd.

Sentek. 2004. Diviner 2000® Portable Soil Moisture Monitoring Solution, User Guide Version 1.21.

Tencate Geosynthetics (2015). Mirafi® H2Ri Woven Geosynthetic for improved Soil Stabilization and Base Course Reinforcement through Continuous Moisture Management. Accessed April 30, 2019, https://www.tencategeo.us/en-us/products/woven-geotextiles/mirafi-h2ri.

Tencate Geosynthetics (2018). Mirafi® RS580i. Accessed April 30, 2019, https://www.tencategeo.us/en-us/products/woven-geotextiles/mirafi-rsi-series.

Wang, F., Han, J., Zhang, X., & Guo, J. (2017). Laboratory tests to evaluate effectiveness of wicking geotextile in soil moisture reduction. *Geotextiles and Geomembranes*, 45(1), 8-13. https://doi.org/10.1016/j.geotexmem.2016.08.002.